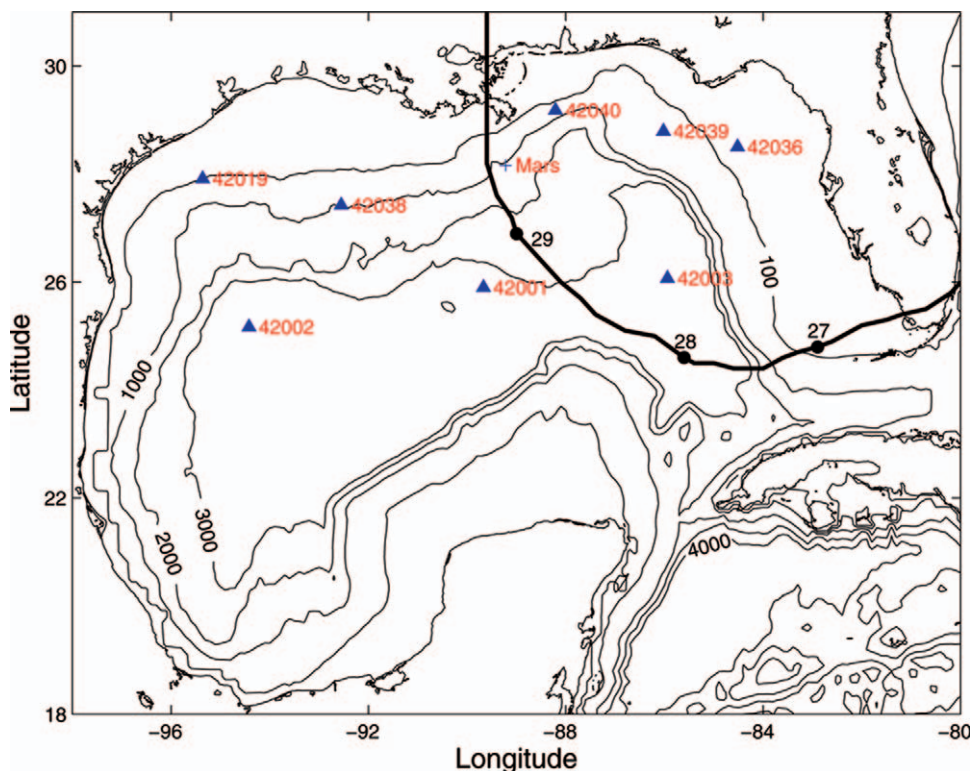


# HINDCAST OF WAVES AND CURRENTS IN HURRICANE KATRINA

BY DONG-PING WANG AND LIE-YAUW O'EY

Extreme wave events during hurricanes can seriously jeopardize the integrity and safety of offshore oil and gas operations in the Gulf of Mexico. Validation of wave forecast for significant wave heights >10 m is critically needed.



**FIG. 1.** The Gulf of Mexico bathymetry map. Katrina's path (solid line) and 0000 UTC-date positions (solid circles) are marked. NDBC buoys (triangles) and Mars platform (cross) also are indicated.

**H**urricane Katrina in 2005 was the costliest and one of the deadliest storms ever to hit the U.S. coast (Knabb et al. 2005). The storm began as a tropical depression over the southeastern Bahamas on 23 August, and was upgraded to Tropical Storm Katrina on 24 August. After crossing southern Florida as a category 1 hurricane, Katrina intensified rapidly over the warm Gulf of Mexico water between 26 and 28 August, and became a category 5 hurricane by 1200 UTC 28 August with maximum

sustained winds of 175 mph. The storm weakened to a category 3 hurricane before making landfall near the Louisiana–Mississippi border at 1100 UTC 29 August. Figure 1 shows the storm track with daily (0000 UTC) positions marked.

Katrina caused extensive damage to offshore oil and gas production facilities; 46 platforms and four jack-up rigs were destroyed. Perhaps most remarkably, Katrina inflicted severe damage on the 36,500-ton Royal Dutch Shell's Mars platform located about

130 miles south of New Orleans, Louisiana in 3,000 ft of water. (The full recovery of Mars production took a year and half and over 1 million man hours.) Mars was the most prolific oil-producing platform in the Gulf of Mexico. Before the storm, it produced 148,000 barrels of oil equivalent per day and 160 million cubic feet of gas. The billion-dollar platform also was designed to withstand “140-mph winds and crashing waves up to 70 ft high simultaneously” (Hays 2007). Less spectacular, but certainly worth noting, was the capsizing of the National Data Buoy Center (NDBC) data buoy 42003, the first loss of a deep-water buoy in the NDBC 30-yr history of operation in the Gulf of Mexico. The record peak significant wave heights of 55 ft at buoy site 42040, a shallow-water buoy located at about 100 miles southeast of New Orleans, also surpassed the record set a year ago at the same buoy during Hurricane Ivan (Panchang and Li 2006). The buoy and platform locations are marked in Fig. 1.

As is true in any extreme storm, while large waves and currents were expected, very few direct surface observations were available during Katrina. For assessing storm damage to offshore facilities, on the other hand, it is essential that the peak wave and current conditions are accurately estimated. In this study, state-of-the-art ocean circulation and surface wave models, driven by wind forcing derived from high-resolution hurricane wind analysis, are used to simulate (hindcast) the ocean states during Katrina. The wave model is validated with buoy and satellite altimetry data. The storm-induced surface currents from the circulation model have not been verified, because at present there is no publicly available information about the surface currents in the path of Katrina.

**MODELS.** The Princeton Regional Ocean Forecast System (PROFS) for the Caribbean Sea and the Gulf

of Mexico (available online at [www.aos.princeton.edu/WWWPUBLIC/PROFS/](http://www.aos.princeton.edu/WWWPUBLIC/PROFS/)) is used to simulate the Loop Current, Loop Current eddy, and upper-ocean wind-driven response. The PROFS is based on the Princeton Ocean Model (POM; Mellor 2004). The model domain includes the entire North Atlantic Ocean, west of 55°W. The model horizontal grid size is variable; it averages about 10 km in the Loop Current and the northwestern Caribbean Sea, and about 5 km in the northeastern Gulf of Mexico (not shown; see Oey and Lee 2002). There are 25 sigma layers, with 10 of them in the upper 10% of the water column. In this study, the model continuously assimilates the satellite sea surface height anomaly (SSHA) from Archiving, Validation, and Interpretation of Satellite Oceanographic Data (AVISO; online at [www.aviso.oceanobs.com](http://www.aviso.oceanobs.com)) and SST from the U.S. Global Ocean Data Assimilation Experiment (GODAE; online at [www.usgodae.org](http://www.usgodae.org)) through 18 August. Thereafter, the model is allowed to run without further injection of satellite data. Surface heat and evaporative fluxes are set to zero. The PROFS has been used for process and hindcast/forecast studies, and has been extensively validated against observations (e.g., Oey et al. 2005; and [www.aos.princeton.edu/WWWPUBLIC/PROFS](http://www.aos.princeton.edu/WWWPUBLIC/PROFS), for a list of other publications). The model recently has been used to study the ocean responses to hurricanes (Oey et al. 2006, 2007; Yin and Oey 2007).

The National Centers for Environmental Prediction (NCEP) Wave Watch III (WW3) (Tolman 2002) is used to model the surface waves. The WW3 is used in operational forecasts (Alves et al. 2005), as well as in process studies (e.g., Moon et al. 2003; Chu et al. 2004); it is a third-generation wave model, which explicitly treats the wave-wave interaction and dissipation due to whitecapping and wave-bottom interaction. In this study the model domain is restricted to the Gulf of Mexico from 14° to 32°N and from 98° to 77°W. The spatial resolution is 0.1° × 0.1°, and the discrete spectrum consists of 36 directions ( $\Delta\theta = 10^\circ$ ) and 34 frequencies (from 0.042 to 1 Hz, with a logarithmic increment). The model incorporates hourly surface currents from PROFS.

The NCEP Global Forecast System (GFS) at present does not adequately resolve the tropical cyclones. In this study, the GFS winds are blended with the National Oceanic and Atmospheric Administration (NOAA)/Hurricane Research Division (HRD) high-resolution analyzed winds (online at [www.aoml.noaa.gov/hrd/](http://www.aoml.noaa.gov/hrd/)). The HRD wind analysis uses all available surface weather observations (e.g., ships, buoys, coastal platforms, surface aviation reports, reconnais-

**AFFILIATIONS:** WANG—School of Marine and Atmospheric Sciences, Stony Brook University, Stony Brook, New York; OY—Atmospheric and Oceanic Sciences, Princeton University, Princeton, New Jersey

**CORRESPONDING AUTHOR:** Prof. Dong-Ping Wang, Ph.D., Marine Sciences Research Center, Stony Brook University, Stony Brook, NY 11794  
E-mail: [dong-ping.wang@stonybrook.edu](mailto:dong-ping.wang@stonybrook.edu)

*The abstract for this article can be found in this issue, following the table of contents.*

DOI:10.1175/BAMS-89-4-487

In final form 26 November 2007  
© 2008 American Meteorological Society

sance aircraft data adjusted to the surface, etc.), and is gridded in a 1000 km × 1000 km moving “box” centered about the hurricane’s track. From HRD winds, storm centers are first linearly interpolated to hourly locations, and consecutive HRD maps are then overlapped at the hourly locations and linearly interpolated. The hourly HRD winds are merged with GFS winds using a weight that retains the HRD data within a circle of radius = 0.8 × side of the box (~400 km), and

smoothly transits into the GFS winds beyond that radius. Figure 2 shows snapshots of GFS + HRD at 0600 UTC 28 August and 0600 UTC 29 August.

Following Oey et al. (2006), the wind stress in PROFS is calculated from the wind using a bulk formula:

$$\begin{aligned}
 C_d \times 10^3 &= 1.2, & |u_a| &\leq 11 \text{ m s}^{-1}; \\
 &= 0.49 + 0.065 |u_a|, & 11 < |u_a| &\leq 19 \text{ m s}^{-1}; \\
 &= 1.364 + 0.0234|u_a| - 0.00023158|u_a|^2, & 19 < |u_a| &< 100 \text{ m s}^{-1},
 \end{aligned}
 \tag{1}$$

where  $|u_a|$  is the wind speed. At present the maximum speed of 100 m s<sup>-1</sup> is adequate, even for intense hurricanes such as Katrina. The formula modifies Large and Pond (1981) to incorporate the limited drag coefficient in high wind speeds (Powell et al. 2003). The wave model, on the other hand, uses the wind as input and calculates the wind stress internally based on a wave boundary layer parameterization (Tolman and Chalikov 1996). The wave model start at 0000 UTC 25 August when Katrina was still a tropical storm near the Bahamas. The hourly model results are saved for the subsequent analysis.

**RESULTS. Currents.** A fast-moving storm such as Katrina excites large inertial currents (Gill 1982). In the northeastern Gulf, the averaged inertial period is about 26 h. To separate rapidly fluctuating iner-

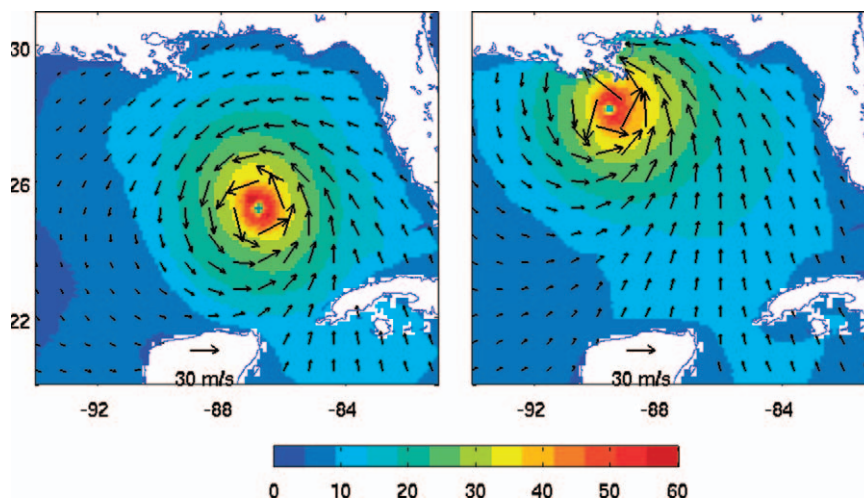
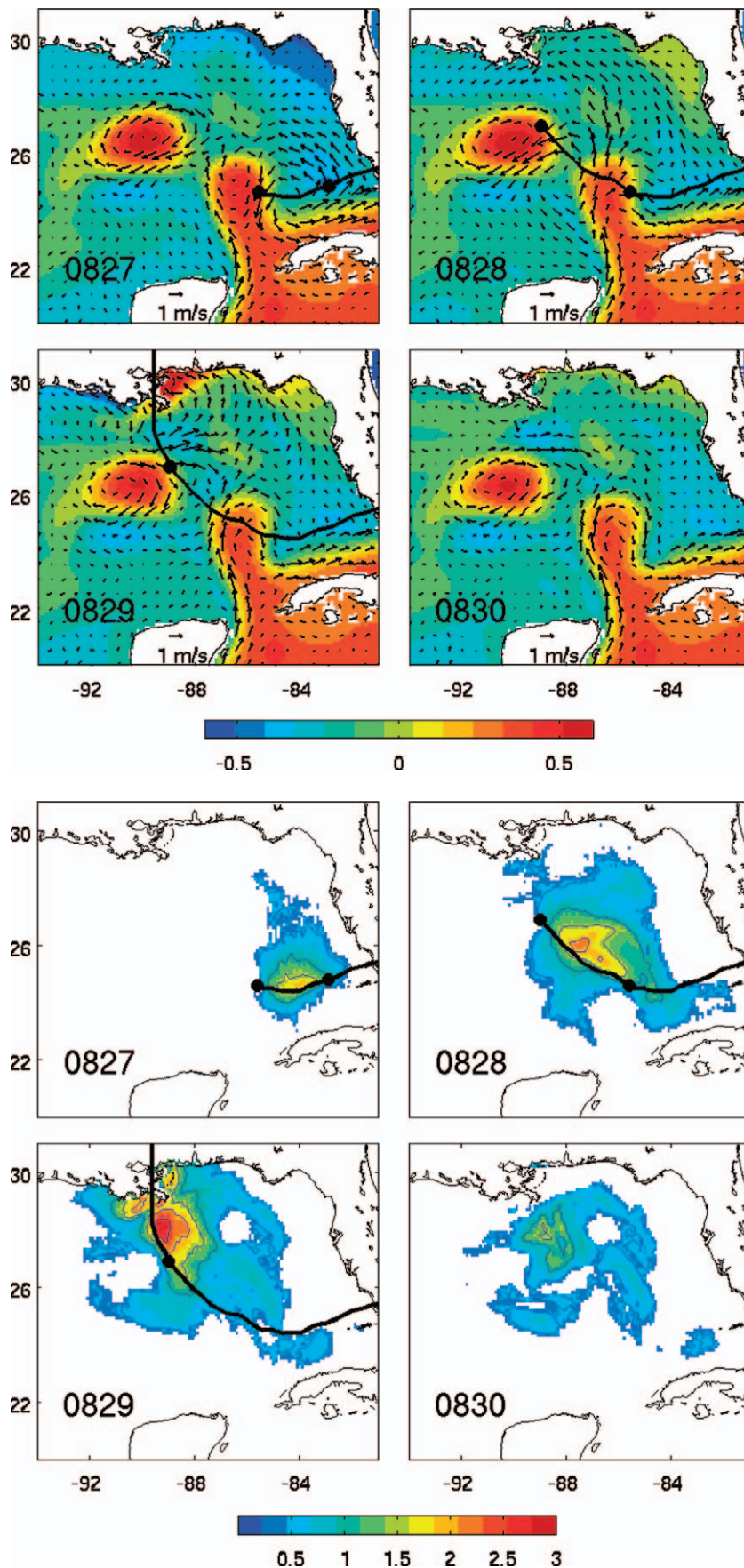


**FIG. 2.** Hurricane Katrina wind vectors (m s<sup>-1</sup>) at (left) 0600 UTC 28 Aug and (right) 0600 UTC 29 Aug from the blended HRD + GFS analysis.

tial motions from otherwise relatively steady currents, the model surface currents are decomposed into the daily mean currents and harmonic-fitted inertial amplitudes. While the filtering of inertial motion using a simple average (box filter) is crude, it is adequate in this application because the mean currents are comparable in magnitude with the inertial currents. Figure 3 shows daily mean currents for 27–30 August with daily mean sea surface heights superimposed. The most conspicuous flow features are the Loop Current and Loop Current eddy, marked by anticyclonic circulations around high sea levels (and a correspondingly deep upper layer). On 28 August, Katrina passed over the Loop Current and Loop Current eddy. Scharroo et al. (2005) suggested that the deep, warm layer was partially responsible for the sudden increase of storm intensity.

Superposed on the Loop Current and Loop Current eddy are large (1–1.5 m s<sup>-1</sup>), transient wind-driven surface currents. The wind-driven currents are frictionally driven and their pattern generally follows the wind. On 27 August the wind-driven currents were concentrated over the west Florida shelf, and on 28 August they were over the northeast of the Loop Current and on the shelves. On 29 August, when Katrina approached the Louisiana and Mississippi coasts, the surface currents had a strong onshore component. The associated large storm surges in Lake Pontchartrain led to the eventual failure of the levee system in New Orleans. (The model-predicted maximum surge height was 4.5 m.)

Figure 4 shows daily inertial amplitudes. Large inertial currents with amplitudes >2 m s<sup>-1</sup> are concentrated under the storm. Unlike the wind-driven



currents, the inertial amplitudes are much larger on the right of the storm path than on the left. The amplitude asymmetry is the consequence of the fast-moving storm. In a stationary storm, the inertial currents, which rotate in a clockwise circle, would be destroyed within a few inertial cycles. In a moving storm, however, the wind vectors turn clockwise on the right side of the storm path (relative to a fixed frame) and turn counterclockwise on the left side. Consequently, the inertial amplitudes are amplified on the right side and suppressed on the left side of the storm. The effect is particularly striking when the wind vectors rotate at about the same rate as the inertial motion (Chang and Anthes 1978; Price 1981).

The inertial motions tend to persist long after the storm has passed. For example, on 30 August large inertial amplitudes ( $\sim 1 \text{ m s}^{-1}$ ) were still present, whereas the wind-driven currents almost completely vanished. We also noted that the inertial currents are considerably smaller ( $< 0.5 \text{ m s}^{-1}$ ) over the Loop Current, the Loop Current eddy, and an anticyclonic eddy north of the Loop Current

**FIG. 3 (above).** Model daily mean surface currents from 27 to 30 Aug. The daily mean sea surface heights (m) are superimposed. (The coastal sea levels on 29 Aug are off the scale; maximum was 4.5 m.) Solid line is the storm path.

**FIG. 4 (left).** Model daily surface inertial amplitudes ( $\text{m s}^{-1}$ ) from 27 to 30 Aug. Only the amplitudes  $> 0.5 \text{ m s}^{-1}$  are shown. Solid line is the storm path.

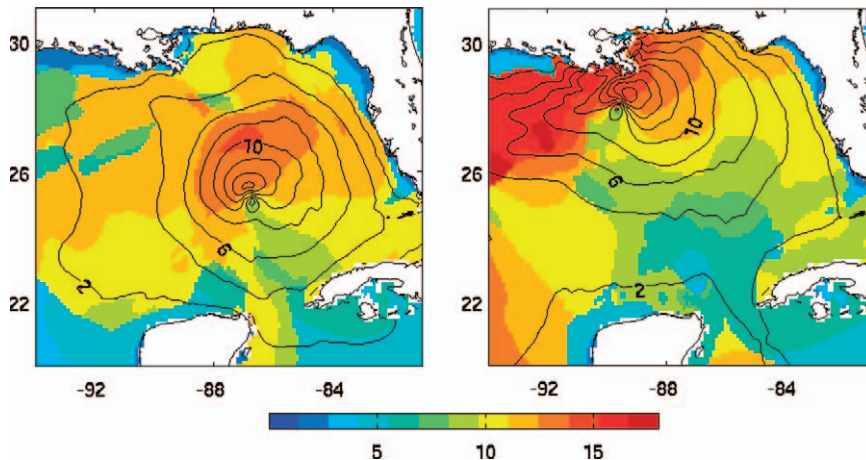


**FIG. 5.** Model significant wave heights (m) and dominant wave periods (s) for (left) 0600 UTC 28 Aug and (right) 0600 UTC 29 Aug.

(Fig. 4). This is consistent with previous observations (Kunze and Sanford 1984) and model studies (Wang 1991), which showed that in regions of strong negative (anticyclonic) vorticity surface inertial energy would rapidly escape below the surface mixed layer. Indeed, after Katrina large inertial currents were found below the mixed layer (G. Forristall 2007, personal communication).

**Waves.** Figure 5 shows snapshots of significant wave heights and dominant wave periods at 0600 UTC 28 August and 0600 UTC 29 August. (Waves are instantaneous values, not the daily averages.) The wave heights are significantly bigger on the right of the storm path. The wind speed, duration, and fetch impact the wave growth. The waves travel with the storm on the right-hand side of the storm path but are away from the storm on the left-hand side. The waves grow much bigger on the right because of the longer fetch. The wave period patterns reveal the directions of wave spreading. The dominant (long period) swells on 28 August were concentrated in the forward direction of the storm, and on 29 August they were toward the west along the coast. Figure 6 shows a swath of maximum wave heights, which are the maximum values of significant wave heights through-

out the hurricane passage. The highest waves are concentrated along the storm path and are biased to the right. The predicted maximum wave heights were over 20 m on 29 August. We note that WW3 is not applicable in the shallow water. When the wave heights are comparable to the water depth, effects such as depth-induced wave breaking and bottom friction become important (Booij et al 1999). Thus, the predicted > 10-m waves along the Louisiana and

Mississippi coasts should not be taken literally. Nevertheless, results from the regional wave model typically are used to specify forcing at the open (seaward) boundaries for a coastal wave model (e.g., Xu et al 2007).

The predicted significant wave heights (Fig. 7) and dominant wave periods (Fig. 8) are compared with NDBC buoy observations (the buoy locations are marked in Fig. 1). The model predictions are excellent at every buoy whether near the storm path or in the western Gulf. Averaged over the storm period (27–30 August), the mean bias is 0.07 m, the mean absolute error is 0.48 m, and the correlation coefficient is 0.97. We note that the model slightly underestimates the maximum wave height at buoy 42040 (15.3 versus 16.9 m), which can be attributed to the large spatial gradient of maximum wave heights

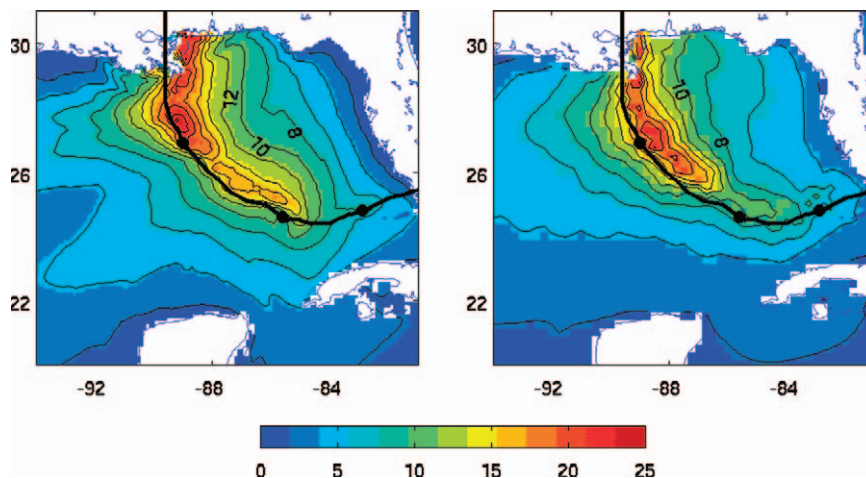


**FIG. 6.** Swath of maximum wave heights (m): (left) this study and (right) NCEP operational model. Solid line is the storm path.

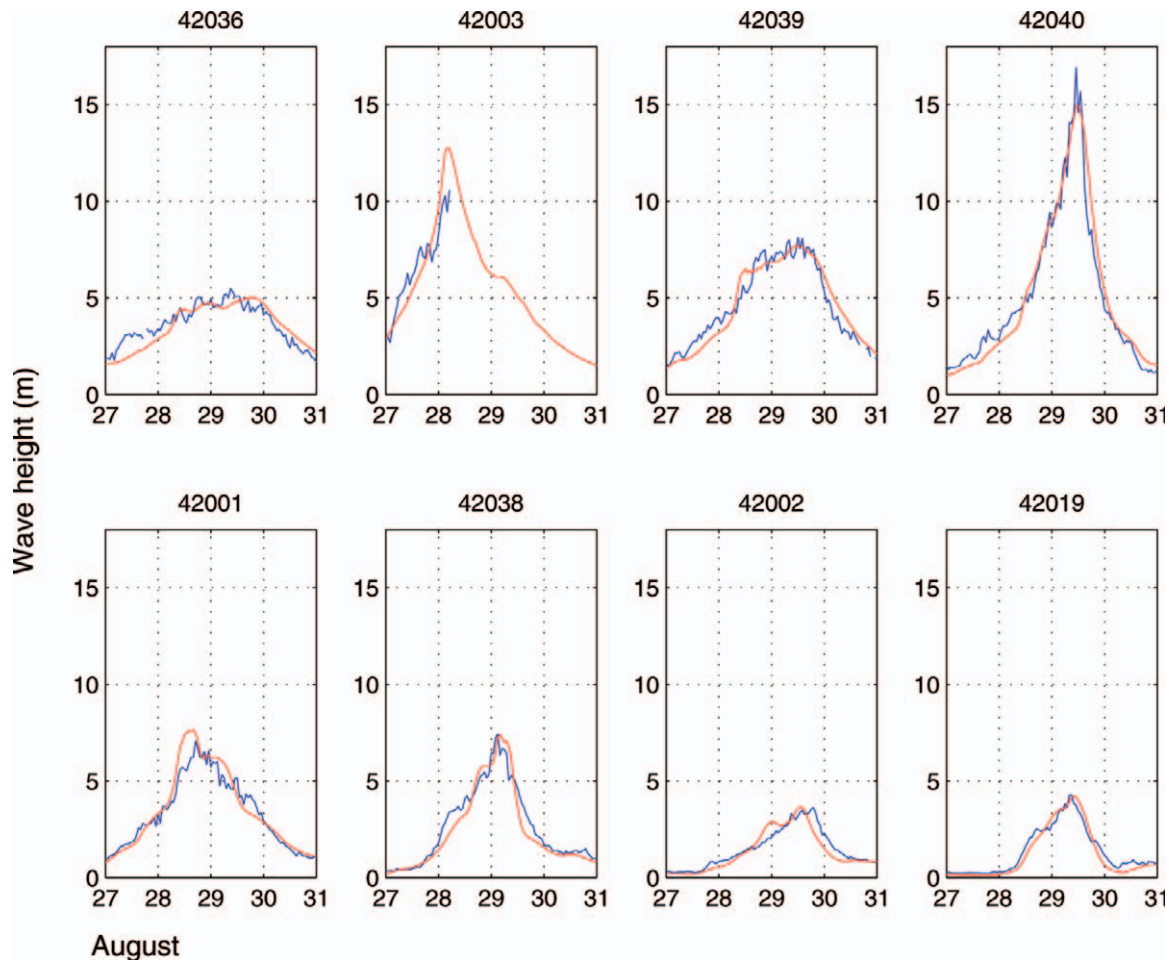


**FIG. 7. Comparison of simulated (red) and observed (blue) significant wave heights at eight NDBC buoys. Buoy locations are marked in Fig. 1.**

in the buoy vicinity (Fig. 6), and perhaps uncertainty in the wind field.

It is interesting to contrast the wave heights between the different buoys. Buoys 42003 and 42040 faced about the same maximum winds (not shown), but the waves were much larger at buoy 42040. The difference is due to the longer fetch, because the waves arriving at buoy 42040 experienced an extra day of the storm forcing. Also, the waves at buoy 42003 were about twice as large as those at buoy 42001, reflecting the bias of larger waves on the right of the storm path. In the western Gulf, the swell conditions are nicely reproduced. For example, at buoy 42019, the first arrival of long-period (>10 s) swells at 0500 UTC 28 August is clearly indicated in the sudden rise of the dominant wave periods (Fig. 8). We also note that the waves only became substantial (>1 m) after 26 August, which indicates that the model initiation (starting on 25 August) has no effect on the results.

Satellite altimetry provides a broad spatial coverage of wave fields. Figure 9 shows all available satellite tracks (28–30 August) in the eastern Gulf during Katrina and a comparison of significant wave heights between the model and altimetry. The model grids are interpolated to the nearest altimetry track. The agreement is excellent (correlation coefficient  $\gamma = 0.96$ ; mean bias = 0.26 m; mean absolute error = 0.46 m). The linear regression line is

$$H_m = 1.13 \times H_s - 0.09, \quad (2)$$

where  $H_m$  and  $H_s$  are, respectively, modeled and satellite significant wave heights (m). The >1 slope is attributed to systematic error in altimetry wave measurements (Tolman 2002). It is also noted that the altimetry is limited to wave heights < 8 m. For larger waves, the altimetry measurements are too scattered to produce meaningful averages and are excluded (AVISO, S. Philipps 2006, personal communication).

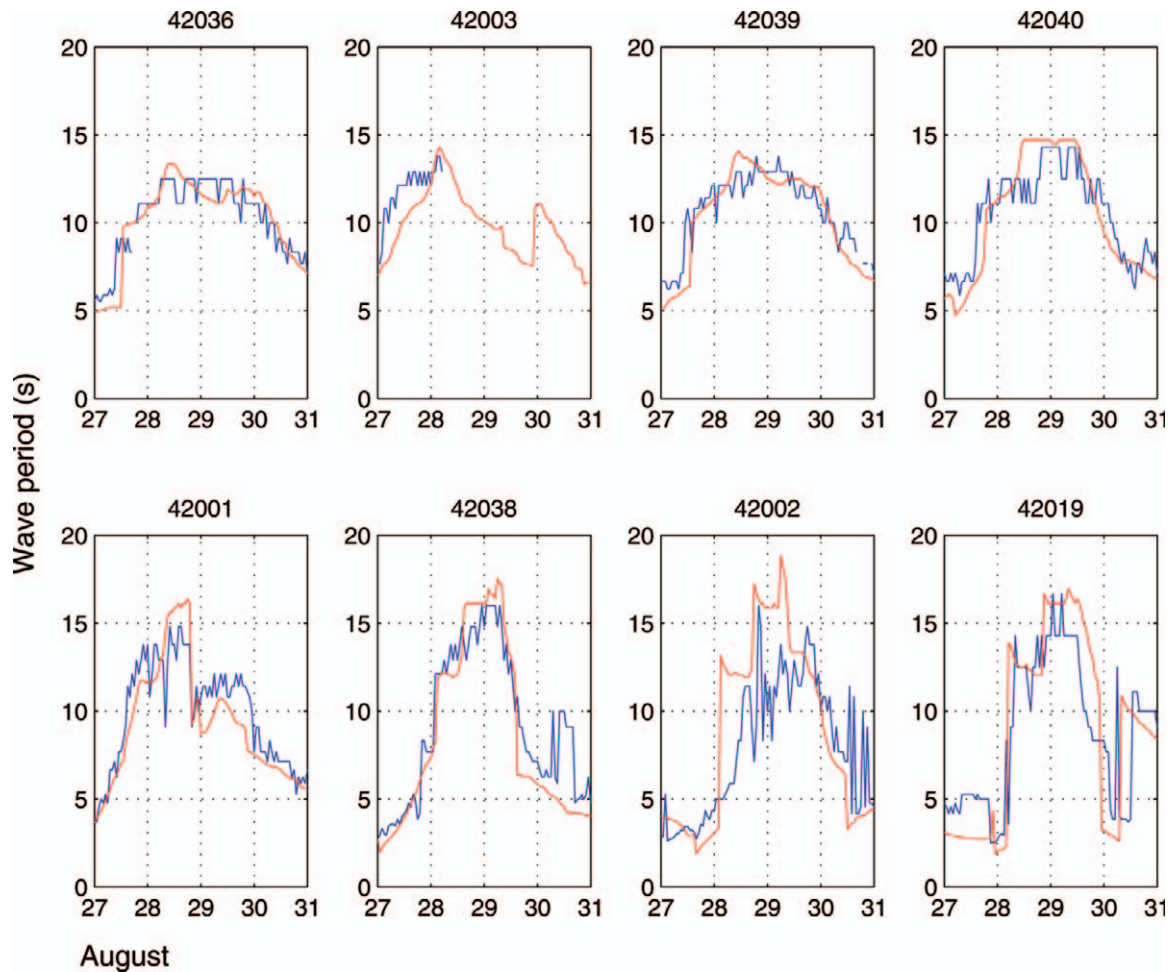


**FIG. 8.** Comparison of simulated (red) and observed (blue) dominant wave periods at eight NDBC buoys. Buoy locations are marked in Fig. 1.

*Comparison with NCEP operational wave model.* The NCEP North Atlantic Hurricane (NAH) regional wave model is based on the same generic WW3 model. The NAH model domain covers the entire North Atlantic Ocean from 0° to 50°N, and from 98° to 30°W. The NAH model resolutions (0.25° × 0.25°, 24 directions and 25 frequencies), however, are much coarser than those used in this study. The NAH model also does not incorporate the surface currents. The wind fields in the NAH model are based on the high-resolution hourly winds from the Geophysical Fluid Dynamics Laboratory (GFDL) hurricane model,

blended with the GFS winds. The 3-hourly NCEP model analyses are obtained (online at <http://polar.ncep.noaa.gov/waves>).

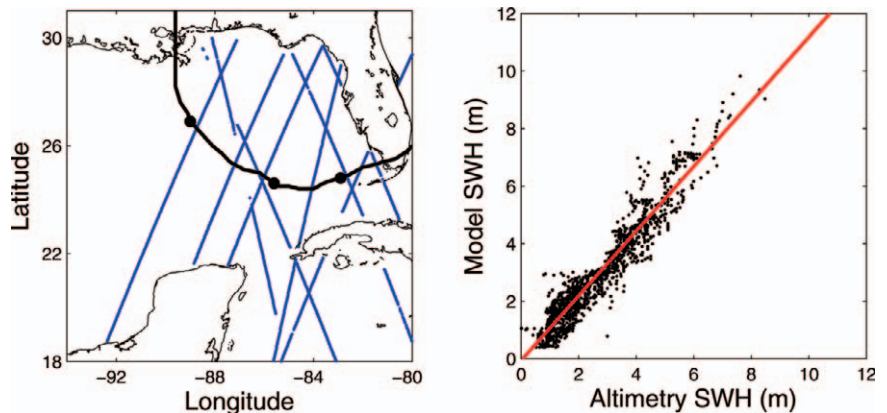


**FIG. 9.** (left) Satellite altimetry tracks during Katrina, and (right) regression of significant wave heights between model and altimetry.

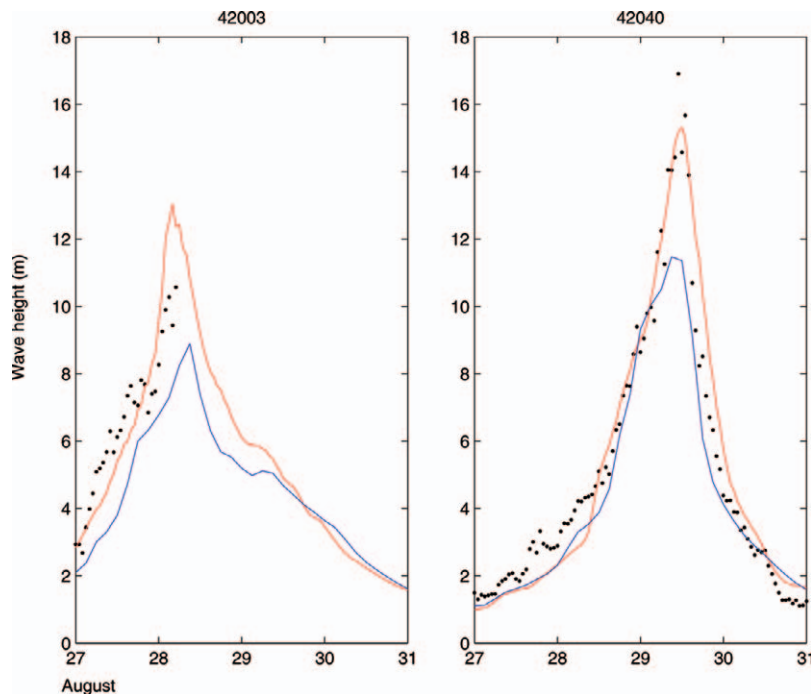


**FIG. 10. Comparison of significant wave heights between this study (red), operational model (blue), and buoy observations (dots) for buoys (left) 42003 and (right) 42040. Buoy 42003 was lost after 0500 UTC 28 Aug.**

In damage assessment the most important parameter is the predicted maximum wave heights. The swath of maximum wave heights from the NAH model is included in Fig. 6 for comparison with our study. The NAH model has a coarser resolution, but its general pattern is similar to that in our study—large waves are concentrated along the storm path and wave heights are biased to the right. The largest wave predicted by the NAH model (22 m) also agrees well with ours (24 m; considering the difference in spatial resolution). However, in the NAH model the large waves are constrained much closer to the storm path. In other words, the spatial extent impacted by the large waves in the NAH model is considerably less (by about 50%) than in our study. This is perhaps best illustrated in comparison of the model predictions at the two buoys (42003 and 42040), which recorded the largest waves. In both cases, the NAH model underestimates the maximum wave heights substantially by as much as 5 m (Fig. 10).

**DISCUSSION.** Extensive damage to offshore oil and gas production facilities during Hurricane Katrina suggest strong combined wind, wave, and current forces. The NDBC buoys, which are few and scattered, are not adequate to map the extreme sea states. In this study, the model simulation

(hindcast) provides a plausible account for the loss of buoys and platforms. Buoy 42003 was capsized when the predicted wave heights reached 13 m (Fig. 7), which exceeded the largest waves ever recorded on buoy 42003 (~11 m; Panchang and Li 2006). The large waves combined with strong winds ( $>32 \text{ m s}^{-1}$ ) and currents might be responsible for this first-ever loss of a deep-water NDBC buoy in the Gulf of Mexico. For the Mars platform, at 0400 UTC 29 August the maximum waves were about 20 m (~66 ft; Fig. 6) and maximum winds were about  $57 \text{ m s}^{-1}$  (~128 mph). (The maximum waves/winds were not at the exact location, but were in the close vicinity.) We do not know the time the Mars superstructure collapsed, but it is probably no coincidence that the predicted sea states had indeed approached

the platform design criterion of simultaneous 70-ft waves and 140-mph winds.

It is well recognized that the drag coefficients used in WW3 are far too large under the hurricane wind condition (Moon et al. 2004). The model success therefore must be partly attributed to careful tuning (Alves et al. 2005). However, because the buoy and altimetry rarely recorded waves  $>10 \text{ m}$ , the wave model has not actually been “validated” for very large waves. In this study, evidence strongly suggests that the predicted large waves were “real.” However, whether WW3 is valid in high wind conditions (when its physics apparently fails) can only be tested by direct measurement of extreme waves in the path of major ( $>$ category 3) hurricanes (e.g., Black et al. 2007). The Gulf of Mexico provides 29% of the domestic oil supply and 19% of the domestic gas production. Accurate marine forecasts of hurricane sea states are of vital interest to the nation’s economic well being.

**ACKNOWLEDGMENTS.** This research is supported by the Minerals Management Service (Contract 1435-01-06-CT-39731). Encouragement from the program manager Dr. Carole Current is appreciated. We thank AVISO for providing the “raw” altimetry records. Computer support from GFDL/NOAA is acknowledged.

## REFERENCES

- Alves, J. H. G. M., Y. Y. Chao, and H. L. Tolman, 2005: The operational North Atlantic hurricane wind-wave forecasting system at NOAA/NCEP. NOAA/NWS/NCEP/MMAB Tech. Note. 244, 59pp.
- Black, P. G., and Coauthors, 2007: Air–sea exchange in hurricanes: Synthesis of observations from the Coupled Boundary Layer Air–Sea Transfer experiment. *Bull. Amer. Meteor. Soc.*, **88**, 357–384.
- Booij, N., R. C. Ris, and L. H. Holthuijsen, 1999: A third-generation wave model for coastal regions, 1. Model description and validation. *J. Geophys. Res.*, **104**, 7649–7666.
- Chang, S. W., and R. A. Anthes, 1978: Numerical simulations of the ocean’s nonlinear baroclinic response to translating hurricanes. *J. Phys. Oceanogr.*, **8**, 468–480.
- Chu, P., Y. Qi, Y. Chen, P. Shi, and Q. Mao, 2004: South China Sea wind-wave characteristics. 1. Validation of Wavewatch-III using TOPEX/Poseidon data. *J. Atmos. Oceanic Technol.*, **21**, 1718–1733.
- Gill, A. E., 1982: *Atmosphere–Ocean Dynamics*. Academic Press, 662 pp, Business section.
- Hays, K., 2007: A survivor in the Gulf: Platform producing more oil than it was when Katrina hit. *Houston Chronicle*, 21 January.
- Knabb, R. D., J. R. Rhome, and D. P. Brown, 2005: Tropical cyclone report, Hurricane Katrina, 23–30 August 2005. National Hurricane Center, 43 pp. [Available online at [www.nhc.noaa.gov/pdf/TCR-AL122005\\_Katrina.pdf](http://www.nhc.noaa.gov/pdf/TCR-AL122005_Katrina.pdf).]
- Kunze, E. and T. B. Sanford, 1984: Observations of near-inertial wave in a front. *J. Phys. Oceanogr.*, **14**, 566–581.
- Large, W. G., and S. Pond, 1981: Open ocean flux measurements in moderate to strong winds. *J. Phys. Oceanogr.*, **11**, 324–336.
- Mellor, G. L., 2004: User’s guide for a three-dimensional, primitive equation, numerical ocean model. Program in Atmospheric and Oceanic Sciences, Princeton University, 42 pp.
- Moon, I.-J., I. Ginnis, T. Hara, H. L. Tolman, C. W. Wright, and E. J. Walsh, 2003: Numerical simulation of sea surface directional wave spectra under hurricane wind forcing. *J. Phys. Oceanogr.*, **33**, 1680–1706.
- , —, and —, 2004: Effect of surface waves on air-sea momentum exchange. Part II: Behavior of drag coefficient under tropical cyclones. *J. Atmos. Sci.*, **61**, 2334–2348.
- Oey, L.-Y., and H.-C. Lee, 2002: Deep eddy energy and topographic Rossby waves in the Gulf of Mexico. *J. Phys. Oceanogr.*, **32**, 3499–3527.
- , T. Ezer, and H. J. Lee, 2005: Loop current, rings and related circulation in the Gulf of Mexico: A review of numerical models and future challenges. *Circulation in the Gulf of Mexico: Observations and Models*, W. Sturges and A. Lugo-Fernandez, Eds., Amer. Geophys. Union, 31–56.
- , —, D. -P. Wang, S. -J. Fan, and X.-Q. Yin, 2006: Loop Current warming by Hurricane Wilma. *Geophys. Res. Lett.*, **33**, L08613, doi:10.1029/2006GL025873.
- , —, —, X.-Q. Yin, and S.-J. Fan, 2007: Hurricane-induced motions and interaction with ocean currents. *Cont. Shelf Res.*, **27**, 1249–1263.
- Panchang, V. G., and D. Li, 2006: Large waves in the Gulf of Mexico caused by Hurricane Ivan. *Bull. Amer. Meteor. Soc.*, **87**, 481–489.
- Powell, M. D., P. J. Vickery, and T. Reinhold, 2003: Reduced drag coefficient for high wind speeds in tropical cyclones. *Nature*, **422**, 279–283.
- Price, J. F., 1981: Upper ocean response to a hurricane. *J. Phys. Oceanogr.*, **11**, 153–175.
- Scharroo, R., W. H. F. Smith, and J. L. Lillibridge, 2005: Satellite altimetry and the intensification of Hurricane Katrina. *Eos, Trans. Amer. Geophys. Union*, **86**, 366.
- Tolman, H. L., 2002: Validation of WAVEWATCH III version 1.15 for a global domain. NOAA/NWS/NCEP/OMB Tech. Note 213, 33 pp.
- , and D. Chalikov, 1996: Source terms in a third-generation wind wave model. *J. Phys. Oceanogr.*, **26**, 2497–2518.
- Wang, D.-P., 1991: Generation and propagation of inertial waves in the Subtropical Front. *J. Mar. Res.*, **49**, 619–633.
- Xu, F., W. Perrie, B. Toulany, and P. C. Smith, 2007: Wind-generated waves in Hurricane Juan. *Ocean Modell.*, **16**, 188–205.
- Yin, X.-Q., and L.-Y. Oey, 2007: Bred-ensemble ocean forecast of Loop Current and rings. *Ocean Modell.*, **17**, 300–326.